Advances in Science and Technology Research Journal

Advances in Science and Technology Research Journal, 2026, 20(6), 149–158
https://doi.org/10.12913/22998624/217190
ISSN 2299-8624, License CC-BY 4.0

Received: 2026.01.03
Accepted: 2026.04.15
Published: 2026.05.01

Assessment of fly ash Nagan Raya as a sustainable supplementary cementitious material

Amir Fauzi[1, 2,*], Rizal Syahyadi[1], Aulia Rachman[2, 3], Muhammad Reza[1, 2], Fajri[1, 2], Mulizar[1, 2], Edi Majuar[1, 2]

[1] Civil Engineering Department, Politeknik Negeri Lhokseumawe, Acheh, Indonesia
[2] Geopolymer and Green Technology Research Centre, Politeknik Negeri Lhokseumawe Acheh, Indonesia
[3] Civil Engineering Department, Universitas Malikussaleh, Acheh, Indonesia
* Corresponding author's e-mail: amirfauzi@pnl.ac.id

ABSTRACT

The by-product produced by the coal-fired power plant in Nagan Raya, Aceh, Indonesia, is referred to as fly ash Nagan Raya (FANR). Based on available characterization data, the particles of FANR exhibited a misty surface texture and contained several key chemical constituents, including Si, Fe, Al, and Ca. Owing to this composition, which closely resembles that of ordinary Portland cement, FANR was a pozzolanic material capable of participating in secondary cementitious reactions that contributed to strength development when combined with a calcium-rich environment. However, FANR absorbed mixing water, leading to reduced consistency and workability of the fresh mortar. The misty surface of the material increased water demand, which in turn influenced the mortar's physical and mechanical properties. As a result, the unique surface characteristics of FANR significantly altered the physical and mechanical properties. The purpose of this study was to assess the qualities of FANR as a cement substitute in mortar. This study examined w/b ratios of 0.55 and 0.50 with FANR incorporated at levels of 5%, 10%, 15%, 20%, and 25%. The study analyzed chemical composition, surface features, setting time, workability, and compressive strength. It found that FANR had a misty surface, spherical particles, and containing Si, Fe, Al, and Ca. In fresh mortar, these properties shortened the setting time and reduced workability. The 28-day compressive strength peaked at a w/b ratio of 0.50 with 5% FANR, and higher FANR levels continued to gain compressive strength beyond 28 days, demonstrating its impact on mortar performance.

Keywords: XRF, XRD, SEM, workability, setting time, compressive strength.

INTRODUCTION

Fly ash, a by-product produced from coal-fired power plants, consists of fine particulate material having a fine particle size. This material was a cementitious substance due to its distinctive chemical composition, which exhibited similarities to that of ordinary Portland cement. The primary oxides presented in fly ash included Ca, Fe, Si, and Al, all of which played essential roles in cementitious reactions (1, 2).

In cement-based systems, fly ash underwent pozzolanic reactions that generated calcium silicate hydrate (C-S-H) and calcium aluminate hydrate (C-A-H) gels (3). These hydration products were essential for improving the strength and durability of cementitious materials by filling voids, binding particles, and refining the microstructure of the hardened binder. Thus, the use of fly ash significantly improved the binder's mechanical properties and long-term stability, while offering a sustainable solution for the reuse of industrial waste materials (4, 5).

Fly ash Nagan Raya (FANR) is an industrial by-product generated from coal combustion at the Nagan Raya power plant in Aceh, Indonesia. This facility played a vital role in supplying electricity to approximately 23 regencies across the provinces of Aceh and North Sumatra. To meet this energy demand, the power plant consumed

around 7000 tonnes of coal per day in 2013 (6). Consequently, the extensive coal consumption generated approximately 15 tonnes of fly ash per day, resulting in substantial environmental and social issues related to waste management, air pollution, and land use.

Characterization results indicated that FANR, much like typical fly ash, was mainly composed of Si, Fe, Al, and Ca oxides, elements that played a crucial role in determining its cementitious and pozzolanic properties. Morphological analysis further indicated that FANR particles exhibited a predominantly spherical shape with a distinctive misty surface texture. These misty, spherical particles resembled regular fly ash but differed slightly in surface morphology, which affected their interaction with water and other components in cementitious systems (7, 8).

The misty surface texture of FANR particles influenced the fresh concrete properties, particularly by decreasing workability, which in turn impacted the increased water absorption. To counteract this effect, the water content in the concrete mixture needed to be adjusted accordingly to maintain consistency and proper flow (9). The chemical interaction between cement and water in freshly mixed mortar acted as the primary binding mechanism, creating the matrix responsible for strength and cohesion. The inclusion of supplementary cementitious materials enhanced these properties by contributing additional reactive components (2). Fauzi et al. reported that the combined oxide content of silicon (Si), iron (Fe), and aluminum (Al) reached 61.71% in Class C fly ash (FA) and 91.35% in Class F FA. In addition, Class C FA contained 27.1% calcium oxide (CaO), whereas Class F FA had only 1.32% CaO (5). These compositional distinctions indicated that Class F FA exhibited higher pozzolanic reactivity than Class C FA, making it more effective for use in concrete production (10).

Supporting this, Isa et al. (11) identified quartz and mullite as the principal crystalline phases in FA. The presence of broad, diffuse humps in the X-ray diffraction (XRD) pattern further indicated substantial amorphous content. The amorphous phase was identified as a key contributor to enhanced cementitious reactivity, as it facilitated the gradual formation of secondary hydration products, notably calcium silicate hydrate (C–S–H) and calcium aluminate hydrate (C–A–H) gels. As hydration progresses, the spherical FA particles become increasingly encapsulated within the developing C–S–H and C–A–H matrices, as demonstrated by subsequent studies (12). This microstructural development played a crucial role in enhancing the long-term strength and durability of the cementitious composite (10).

Typically, fly ash particles exhibited a spherical morphology, consisting predominantly of smooth, glassy microspheres formed through the rapid solidification of molten mineral matter during combustion (1). The spherical shape enhanced the workability of cementitious mixtures by acting as micro ball bearings, reducing internal friction and improving particle packing density (13). In addition to solid spheres, other morphological forms such as cenospheres (hollow spheres) and plerospheres (large spheres containing smaller ones) were often observed (14). These hollow, porous particles lowered the overall bulk density and influenced both the mechanical and rheological behavior of fly ash–based materials.

Scanning electron microscopy (SEM) revealed that Class F fly ash obtained from bituminous coal is predominantly composed of smooth, dense, fine spherical particles with a relatively uniform size distribution (1). In contrast, Class C fly ash produced from sub-bituminous coal generally contains spherical, partially fused particles, often accompanied by crystalline residues such as lime (1). These morphological variations were strongly associated with differences in chemical composition, especially the calcium oxide (CaO) content, which governed the reactivity and hydration behavior of the fly ash in cementitious systems (1).

Furthermore, the amorphous glassy phase surrounding the fly ash particles was a key contributor to their pozzolanic reactivity. The smooth surfaces of the spherical particles provided fewer nucleation sites for early hydration products. Nevertheless, they supported the gradual dissolution of reactive silica (SiO_2) and alumina (Al_2O_3), which in turn promoted the formation of secondary hydration products, including calcium silicate hydrate (C–S–H) and calcium aluminate hydrate (C–A–H) gels (15, 16). Over time, these gels gradually filled the interparticle voids, resulting in a denser matrix and improved compressive strength (17).

As a supplementary cementitious material, fly ash influenced cement hydration kinetics through its physical properties, chemical makeup, and pozzolanic activity. In general, incorporating fly ash tended to prolong both the initial and final

setting times compared with ordinary Portland cement (OPC) mortar (18, 19). This delay resulted from the relatively slow pozzolanic reaction of fly ash compared with the rapid hydration of Portland cement. In the initial stages, fly ash showed low reactivity since the dissolution of amorphous silica (SiO_2) and alumina (Al_2O_3) required a strongly alkaline environment that developed gradually with the release of calcium hydroxide ($Ca(OH)_2$) during cement hydration (1,20). As a result, the formation of early hydration products such as calcium silicate hydrate (C–S–H) and calcium aluminate hydrate (C–A–H) gels prolonged the setting time (21).

The type and chemical makeup of fly ash strongly affected its impact on the setting time behavior. Class F fly ash, which contained low calcium oxide (CaO) and high amounts of amorphous silica and alumina, generally produced a more substantial delay in setting time because of its slower pozzolanic reaction (1). In contrast, Class C fly ash, characterized by a higher CaO content and self-cementing behavior, accelerated the setting time through additional hydration reactions between CaO and water (10). The reactive calcium phases, such as free lime found in Class C fly ash, promoted quicker formation of C–S–H and ettringite, which in turn shortened the setting time (22).

Moreover, particle size and fineness also played a critical role. Finer fly ash particles enhanced reactivity by increasing surface area, promoting faster dissolution and reaction with calcium hydroxide. Previous studies reported that mechanical activation of fly ash substantially decreased setting time while increasing early compressive strength (23). However, excessive replacement levels of cement with fly ash (>30%) generally led to a noticeable delay, especially under low curing temperatures (24). Additionally, the mortar exhibited initial and final setting times of up to 260 minutes and 315 minutes, respectively, due to the high fly ash content and the 35–50% replacement level (25).

In general, fly ash contributed to improving mortar workability, depending on its classification, particle shape, fineness, and the proportion employed as a replacement material (1, 26, 27). Studies indicated that fly ash, especially Class F, was predominantly composed of smooth, glassy spherical particles that function as microscopic "ball bearings" within the mixture (28). This ball-bearing effect reduced internal friction among solid particles, allowing the mortar to flow more easily and requiring less water to achieve a given level of consistency (13). Consequently, incorporating fly ash enhanced the flowability and lowered water demand, offering advantages for both the mixing process and the resulting microstructure.

The fineness and particle size distribution of fly ash also significantly affected its impact on workability. Finer fly ash particles occupied the voids between cement grains, enhancing particle packing and lowering water demand through the "filler effect" (29). However, if the fly ash was too fine or used at a very high replacement level, it increased the surface area of solids in the mix, thereby increasing water demand and slightly reducing workability (30).

Studies revealed a non-linear impact of fly ash replacement on workability (31, 32). Superplasticizers increased the workability of fly ash mortar by improving cement dispersion and admixture performance (33). Fly ash improved workability by lowering the heat of hydration and setting time, while enhancing cohesion and uniformity (32, 34). According to a different study, the workability was reduced by FA up to 20% of the cement replacement. Nonetheless, increasing the FA content from 20% to 40% in the cement replacement improved the workability.

The influence of fly ash on mortar compressive strength has been widely investigated, with findings consistently indicating lower early-age strength but substantial strength gains at later ages. This behavior stemmed from the slower pozzolanic reaction of fly ash compared with Portland cement hydration (35). Class F fly ash, characterized by low calcium content and high levels of silica (SiO_2) and alumina (Al_2O_3), typically delivers lower early strength due to its limited self-cementing properties. Nevertheless, it provides substantial long-term strength gains as pozzolanic reactions gradually generate additional calcium silicate hydrate (C–S–H) and calcium aluminate hydrate (C–A–H) gels that refine and densify the microstructure (30, 36). In contrast, Class C fly ash, owing to its higher calcium content, typically improves early-age strength due to its inherent hydraulic reactivity and also contributes to long-term strength through ongoing secondary hydration (10).

Several researchers reported that the level of cement replacement played a crucial role in determining compressive strength performance.

Moderate (15–30%) fly ash replacement maintained or improved 28-day strength, while higher levels (>40%) reduced early strength (23,37). Compressive strength was affected by particle fineness and curing conditions. Higher fly ash fineness enhanced reactivity via increased surface area, and elevated curing temperatures accelerated pozzolanic reactions, leading to improved long-term strength (38,39).

With a compressive strength of up to 35% after 365 days, the ideal cement replacement in the mortar was 50% FA (40). An increase in fly ash content also resulted in lower compressive strength at 28 days. However, by 180 days, the strength gradually improved, even with cement replacement levels of up to 40% (41). These findings correspond to typical fly ash, which featured a glassy surface and spherical particle morphology (1). The surface and shape of general fly ash and FANR were the points of difference characteristic of the material. The material of FANR as a substitute for cement, however, was not sufficiently described. Therefore, the FANR was used in the current investigation to substitute for cement in the mortar's properties.

MATERIALS AND METHOD

Mortar mixtures incorporating fly ash from Nagan Raya, Indonesia (FANR), referred to ASTM C305 (42). The Portland composite cement (PCC) was the comparable material in this study. The mix of dry materials was for 60 seconds before the addition of water, followed by low and high speed mixing, with a final 60 seconds after a brief scraping interval. Mortar specimens were demolded after 24 h and subsequently water-cured. A total of 48 cube specimens were prepared with w/b ratios of 0.50 and 0.55 and tested for compressive strength at curing ages of 1, 3, 7, and 28 days, with three specimens tested at each age.

ASTM C1437 mentioned the measure of workability using the flow table test in accordance with ASTM C1437 (43). The mortar was placed into the mold in two layers, each compacted with 20 tamps, followed by mold removal and 25 table drops within 15 s. The workability was on the average spread diameter in two perpendicular directions. The initial and final setting times of the binder paste were measured using the Vicat apparatus in accordance with ASTM C191 (44). The Vicat needle penetrated to 25 ± 2 mm from the bottom of the mold, which determined the initial setting. The absence of a visible impression on the paste surface, with time measured from the initial contact between water and binder, determined the final setting time.

RESULTS AND DISCUSSION

Chemical composition

Based on previous data, FANR exhibited cementitious characteristics because its chemical composition supported the formation of C–S–H and C–A–H gels. As shown in Table 1, PCC contained 14.22% SiO_2, 4.11% Al_2O_3, 2.72% Fe_2O_3, and 73.86% CaO. In comparison, FANR consisted of 48.04% SiO_2, 27.62% Al_2O_3, 11.78% Fe_2O_3, and 6.44% CaO. The substantially higher SiO_2 and Al_2O_3 contents in FANR compared with PCC suggest a strong pozzolanic potential. FANR reacts with calcium hydroxide to produce calcium silicate hydrate (C–S–H) and calcium aluminate hydrate (C–A–H), contributing to long-term compressive strength, setting time, and early strength development.

Additionally, FANR contains more Fe_2O_3 than PCC, which influences both compressive strength and binder coloration. However, its CaO content is lower than that of PCC, the key component driving cement hydration and compressive strength. This lower CaO content makes FANR suitable as a supplementary cementitious material when blended with PCC. Both materials also exhibit low LOI values, reflecting minimal volatile matter such as moisture. The FANR chemical composition results were consistent with previous findings (11).

Identification material and binder

The materials and binders at w/b ratios of 0.55 and 0.50 were analyzed using XRD. Figure 1 reveals a prominent peak at approximately 29° (2θ) in PCC, corresponding to well-defined crystalline phases, including calcite ($CaCO_3$) and C_3S/C_2S. Meanwhile, FANR exhibits peaks corresponding to quartz, mullite, and hematite, reflecting its high pozzolanic potential due to the presence of reactive aluminosilicate phases. FANR is also notably rich in crystalline aluminosilicates.

Table 1. Chemical composition of PCC and FANR

Chemical composition in Oxide	Percentage weight	
	PCC	FANR
SiO_2	14.22	48.04
Al_2O_3	4.11	27.62
Fe_2O_3	2.72	11.78
CaO	73.86	6.44
MnO	0.09	0.21
K_2O	0.85	0.98
LOI	4.94	4.15

The conventional binder exhibits a more amorphous matrix than the crystalline structure of FANR, consistent with the presence of typical cement hydration products such as C–S–H and ettringite. The broad peak between 25° and 35° 2θ indicates a higher proportion of amorphous material, suggesting extensive reaction between FANR and $Ca(OH)_2$ to form amorphous pozzolanic products.

Figure 1b shows that the conventional binder with a w/b ratio of 0.50 also contains amorphous C–S–H, accompanied by moderate peaks representing unreacted components. In contrast, the FANR binder exhibits greater crystallinity, with clear peaks corresponding to quartz, mullite, and hematite. These findings align with the results reported by Isa et al. (11), who similarly identified quartz and mullite as key crystalline constituents of FANR.

Image of material and binder

Figure 2 presents the particle and binder morphologies at w/b ratios of 0.55 and 0.50. The PCC image in Figure 2a shows a heterogeneous matrix containing large, irregular flakes measuring approximately 10–20 µm. These flakes contribute to the formation of hydrated cement paste. PCC also exhibits a rough and porous surface, reflecting ongoing hydration. Furthermore, FANR powder in Figure 2b, by contrast, displays a spherical, fibrous structure with a heterogeneous, misty amorphous appearance. Its particle size is generally below 5 µm. The morphology of the FANR binder at a w/b ratio of 0.50 is in Figure 2c. It exhibits a densely packed granular surface characterized by rounded agglomerates and a rough texture. This morphology indicates substantial pozzolanic activity and the presence of secondary hydration products such as C–S–H (calcium silicate hydrate), C–A–H (calcium aluminate hydrate), and ettringite. The rough particle surfaces suggest that FANR reacted to form cementitious gels, while the smoother particle transitions reflect strong bonding within the binder.

Additionally, Figure 2d indicates that the reaction between FANR and $Ca(OH)_2$ facilitates the formation of additional C–S–H gel, resulting in a denser microstructure and enhanced long-term strength and durability. The morphology of the FANR binder at a w/b ratio of 0.50 shows a moderately dense matrix with spherical particles and a rough surface. This moderate density is associated with reduced early-age strength and durability. Incomplete gel coverage indicates the presence of unreacted FANR and residual calcium hydroxide, and the less consolidated surfaces suggest limited secondary C–S–H formation. Previous investigations described conventional fly ash as having a glassy, spherical particle

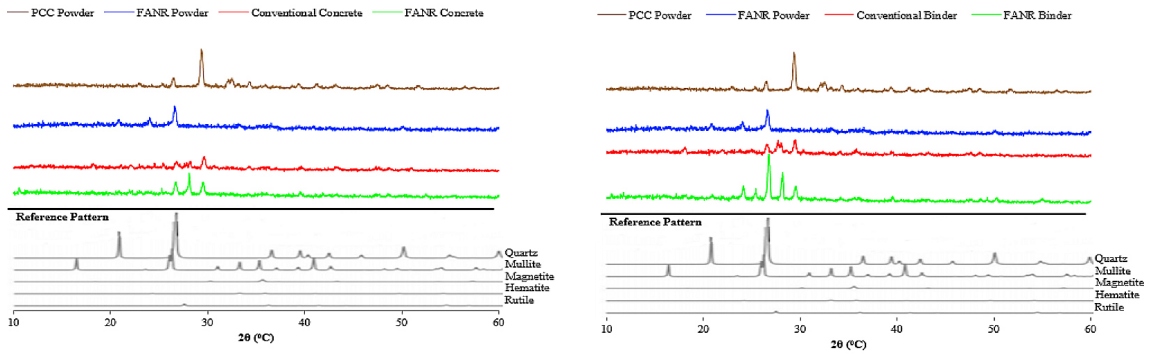

(a) XRD pattern in the w/b of 0.55 (b) XRD pattern in the w/b of 0.50

Figure 1. The identification of material of PCC, FANR, conventional binder, and FANR binder with the w/b ratio of 0.55 and 0.50

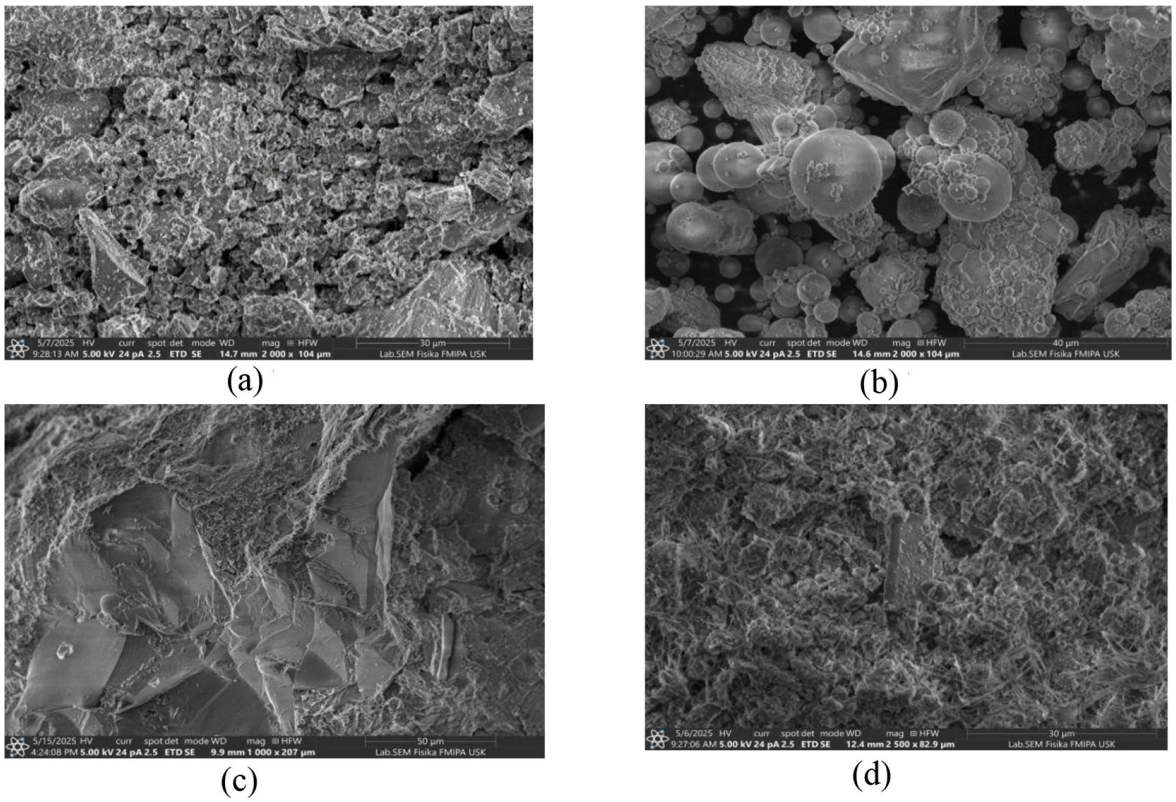

Figure 2. The characteristic of morphology: (a) the powder of PCC, (b) the powder of FANR, (c) the FANR paste with w/b ratio of 0.55, (d) the FANR paste with w/b ratio of 0.50

morphology (12). It highlighted the distinct contrast with FANR.

Workability

In this study, the workability of fresh FANR mortar was evaluated at a w/b ratio of 0.55 and 0.50, respectively. Figure 3 shows that the increase in FANR content caused a higher superplasticizer and reduced w/b ratios. As FANR content increased, more superplasticizer was needed to maintain workability. It was attributed to the higher surface area and misty texture of FANR particles, increasing the water demand. Similarly, the mixture with a lower w/b ratio of 0.50 required more superplasticizer than the 0.55 mixture to achieve comparable workability, indicating that reduced water content naturally produces stiffer mixes that rely more on chemical admixtures.

At this ratio, the FANR mortar exhibited a significant reduction in workability. The higher water demand was attributed to the misty particle surfaces, which absorbed more water. This behavior contrasts with the findings of Zhang (25), who reported enhanced workability with increasing fly ash content, likely due to differences in surface characteristics between the FANR used in this study and the fly ash investigated in earlier research.

Setting time

Figure 4 presents the setting time behavior of FANR mortar at a w/b ratio of 0.55. The modified chemical composition had a pronounced effect on setting time. As FANR content increased, the setting time decreased. This reduction occurred because the misty surface of FANR particles absorbed water from the fresh mix, causing it to dry more rapidly. Additionally, the relatively high calcium content in FANR contributed to accelerated early hydration, further shortening the setting time.

The mortar with a w/b ratio of 0.55 exhibited a slightly longer setting time than the mixture with a ratio of 0.50, indicating that higher water content delays setting slightly by diluting the cementitious reactions. Overall, the results suggest a clear relationship between workability and setting time; mixtures that remain workable for longer generally exhibit longer setting times, and vice versa. These findings align with

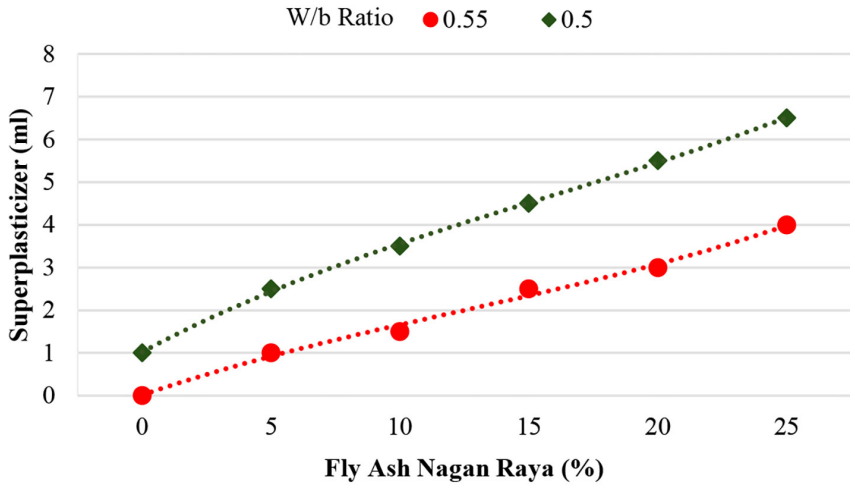

Figure 3. Workability with the w/b ratio of 0.55 and 0.50

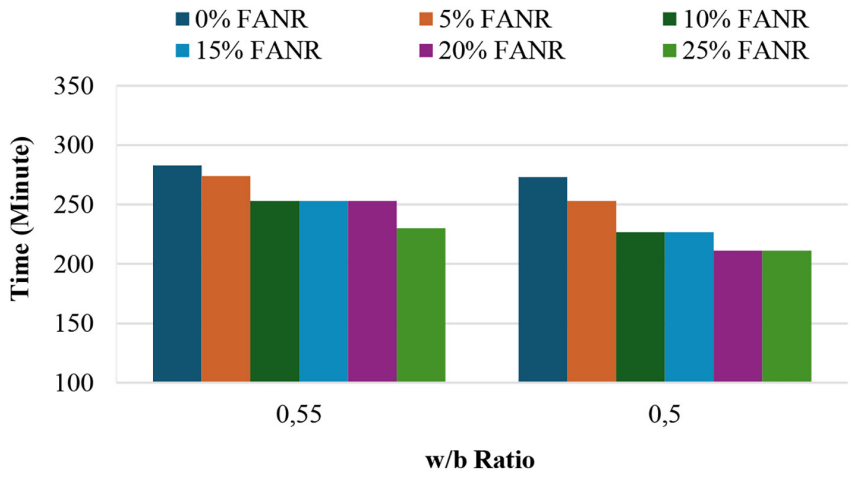

Figure 4. Setting time with the w/b ratio of 0.55 and 0.50

Zhang's report, which showed that replacing 35–50% of cement with fly ash resulted in initial and final setting times of 260 and 315 minutes, respectively (25).

Compressive strength

Figures 5 and 6 show the compressive strength results for w/b ratios of 0.55 and 0.50. Figure 5 shows the compressive strength at 1, 3, 7, and 28 days for FANR replacement levels of 5%, 10%, 15%, 20%, and 25% at a w/b ratio of 0.55. The 28-day compressive strength curve reveals a clear pattern in which the pozzolanic reaction in FANR mortar became more pronounced after 28 days, unlike in the conventional binder. This enhanced pozzolanic activity involved reactive components that accelerated hydration over time. The increased reaction rate was further supported by FANR's fine particle size and larger surface area.

Figure 6 shows the compressive strength at 1, 3, 7, and 28 days for FANR replacement levels of 5%, 10%, 15%, 20%, and 25% at a w/b ratio of 0.50. The conventional mortar achieved the highest compressive strength, indicating optimal compressive strength without the need for cement replacement. The 5% FANR mix performed similarly to the control and continued to exhibit strong compressive strength development, particularly beyond 28 days.

Cement replacement levels below 15% maintained relatively good compressive strength. However, the mechanical performance, especially compressive strength, was affected at low w/b ratios due to the misty surface of FANR, which absorbed more water from the fresh mixture. FANR replacement up to 20%

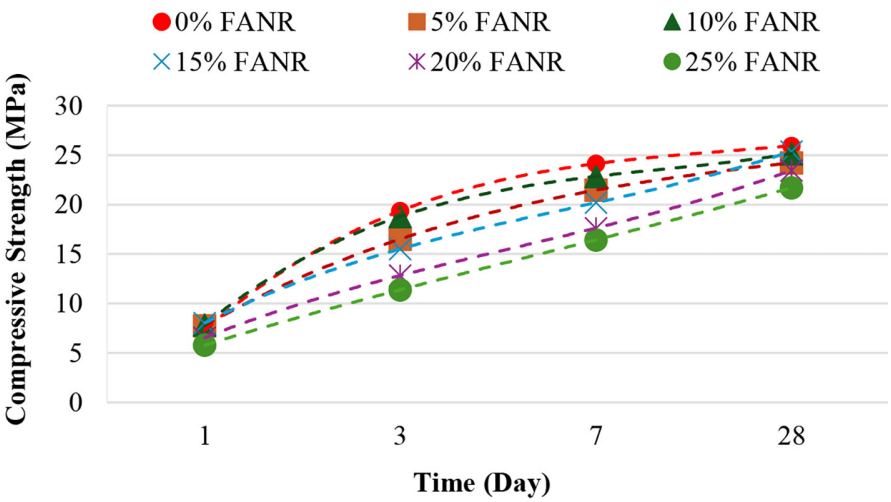

Figure 5. Compressive strength with the w/b ratio of 0.55

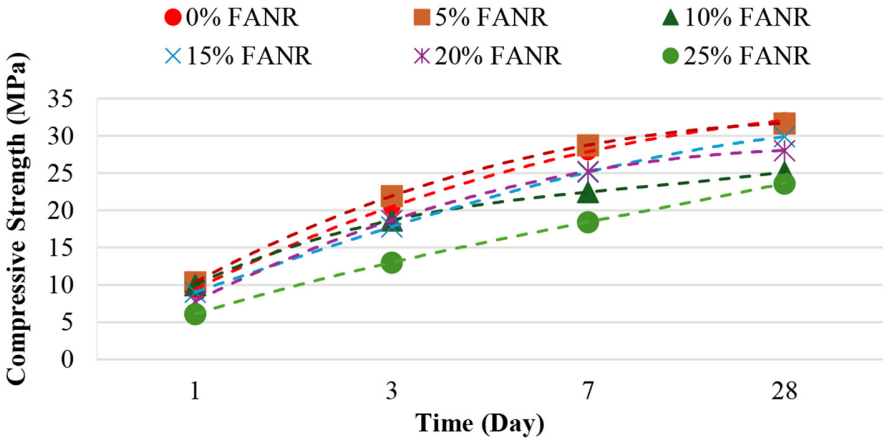

Figure 6. Compressive strength with the w/b ratio of 0.50

resulted in lower early compressive strength compared to the control. However, the mixes continued to gain compressive strength at later ages. These findings are consistent with earlier studies reporting increased long-term strength in fly ash blended systems (40).

CONCLUSION

FANR showed strong pozzolanic potential due to its high SiO_2, Al_2O_3, and Fe_2O_3 contents, which supported the formation of C–S–H and C–A–H gels. Although its lower CaO content limited early hydration, it contributed to considerable long-term strength development when used as a partial cement replacement. Mineralogical and morphological analyses confirmed the presence of reactive aluminosilicate phases and a fine, porous texture that enhanced pozzolanic activity but increased water demand. Furthermore, FANR reduced workability and accelerated setting time because of its misty and high surface area, requiring higher superplasticizer dosages. At 28 days, the mixture with 5% FANR replacement achieved the highest compressive strength, while higher replacement levels continued to show strength gains beyond 28 days.

Acknowledgment

The authors express their gratitude to the Endowment Fund for the Education Agency of Indonesia for this research. Appreciation is also extended to the Nusantara Power plant in Nagan Raya for providing material access, as well as to the Nagan Raya local government for facilitating field application activities.

REFERENCES

1. Alterary SS, Marei NH. Fly ash properties, characterization, and applications: A review. J King Saud Univ Sci. 2021 Sep 1;33(6).
2. Li G, Zhou C, Ahmad W, Usanova KI, Karelina M, Mohamed AM, et al. Fly ash application as supplementary cementitious material: A review. Materials. 2022 Apr 1;15(7).
3. Luhar I, Luhar S. A comprehensive review on fly ash-based geopolymer. Journal of Composites Science. 2022 Aug 1;6(8).
4. ASTM. Standard Specification for Coal Fly Ash and Raw or Calcined Natural Pozzolan for Use in Concrete. 2014;C 618:1–5.
5. Fauzi A, Nuruddin MF, Malkawi AB, Abdullah MMAB. Study of fly ash characterization as a cementitious material. In: Procedia Engineering. Elsevier Ltd; 2016; 487–493.
6. PwC Indonesia. Power In Indonesia Investment and Taxation Guide. 2018. Available from: www.pwc.com/id
7. Fauzi A, Majuar E, Jufriadi, Syukri, Rachman A. Geopolimer sebagai alternatif semen pada masa datang. Risanto E. (Ed.) Yogyakarta: Penerbit Andi; 2023; 1–53.
8. Ruhana, Fauzi A, Syahyadi R, Fajri, Rachman A, Fazliah, et al. The Influence of NaOh Solution on The Efflorescence of Geopolymer Mortar. In: AIP Conference Proceedings. American Institute of Physics Inc.; 2023.
9. Fauzi A, Syukri, Mulizar, Reza M. Feasibility of utilization EAFD as cement replacement in conventional concrete. Jurnal Teknik Sipil. 2017;9(1).
10. Akbulut ZF, Yavuz D, Tawfik TA, Smarzewski P, Guler S. Enhancing concrete performance through sustainable utilization of class-c and class-f fly ash: a comprehensive review. Sustainability (Switzerland). 2024 Jun 1;16(12).
11. Isa FN, Johari MAM, Anum I, Agabus JL, Soji SM, Salihu CH. Performance of high strength concrete containing locust bean pod ash as cement replacement. Research on Engineering Structures and Materials. 2024;10(1):71–89.
12. Shahsavari R, Hwang SH. Morphogenesis of cement hydrate: from natural C-S-H to synthetic C-S-H. In: Cement Based Materials. InTech; 2018.
13. Ulusoy U. A review of particle shape effects on material properties for various engineering applications: From Macro to Nanoscale. Minerals. 2023 Jan 1;13(1).
14. Shishkin A, Abramovskis V, Zalite I, Singh AK, Mezinskis G, Popov V, et al. Physical, thermal, and chemical properties of fly ash cenospheres obtained from different sources. Materials. 2023 Mar 1;16(5).
15. Camerini R, Poggi G, Ridi F, Baglioni P. The kinetic of calcium silicate hydrate formation from silica and calcium hydroxide nanoparticles. J Colloid Interface Sci. 2022 Jan 1;605:33–43.
16. Barzgar S, Yan Y, Tarik M, Skibsted J, Ludwig C, Lothenbach B. A long-term study on structural changes in calcium aluminate silicate hydrates. Mater Struct. 2022 Dec 1;55(10).
17. Nana A, Cyriaque Kaze R, Salman Alomayri T, Suliman Assaedi H, Nemaleu Deutou JG, Ngouné J, et al. Innovative porous ceramic matrices from inorganic polymer composites (IPCs): Microstructure and mechanical properties. Constr Build Mater. 2021 Mar 1;273.
18. Nedunuri SSSA, Sertse SG, Muhammad S. Microstructural study of Portland cement partially replaced with fly ash, ground granulated blast furnace slag and silica fume as determined by pozzolanic activity. Constr Build Mater. 2020 Mar 30;238.
19. Mohamed OA, Najm O, Ahmed E. Alkali-activated slag & fly ash as sustainable alternatives to OPC: Sorptivity and strength development characteristics of mortar. Cleaner Materials. 2023 Jun 1;8.
20. Panda L, Dash S. Characterization and utilization of coal fly ash: A review. Emerging Materials Research. ICE Publishing; 2020; 9: 921–34.
21. Al-saffar FY, Wong LS, Paul SC. An elucidative review of the nanomaterial effect on the durability and calcium-silicate-hydrate (C-S-H) gel development of concrete. Gels. 2023 Aug 1;9(8).
22. Aldawsari S, Kampmann R, Harnisch J, Rohde C. Setting time, microstructure, and durability properties of low calcium fly ash/slag geopolymer: A review. Materials. 2022 Feb 1;15(3).
23. Shah SFA, Chen B, Oderji SY, Haque MA, Ahmad MR. Improvement of early strength of fly ash-slag based one-part alkali activated mortar. Constr Build Mater. 2020 Jun 20;246.
24. Zhang H, Li L, Yuan C, Wang Q, Sarker PK, Shi X. Deterioration of ambient-cured and heat-cured fly ash geopolymer concrete by high temperature exposure and prediction of its residual compressive strength. Constr Build Mater. 2020 Nov 30;262.
25. Zhang MH, Sisomphon K, Ng TS, Sun DJ. Effect of superplasticizers on workability retention and initial setting time of cement pastes. Constr Build Mater. 2010 Sep;24(9):1700–7.
26. Seifan M, Mendoza S, Berenjian A. Mechanical properties and durability performance of fly ash based mortar containing nano- and micro-silica additives. Constr Build Mater. 2020 Aug 20;252.
27. Seifan M, Mendoza S, Berenjian A. A comparative study on the influence of nano and micro particles on the workability and mechanical properties of mortar supplemented with fly ash. Buildings. 2021 Feb 1;11(2):1–17.

28. Sun J, Zhang Z, Hou G. Utilization of fly ash microsphere powder as a mineral admixture of cement: Effects on early hydration and microstructure at different curing temperatures. Powder Technol. 2020 Sep 20;375:262–70.
29. Saradar A, Rezakhani Y, Rahmati K, Johari Majd F, Mohtasham Moein M, Karakouzian M. Investigating the properties and microstructure of high-performance cement composites with nano-silica, silica fume, and ultra-fine TiO_2. Innovative Infrastructure Solutions. 2024 Apr 1;9(4).
30. Ram AK, Mohanty S. State of the art review on physiochemical and engineering characteristics of fly ash and its applications. Int J Coal Sci Technol. 2022 Dec 1;9(1).
31. Chindaprasirt P, Kroehong W, Damrongwiriyanupap N, Suriyo W, Jaturapitakkul C. Mechanical properties, chloride resistance and microstructure of Portland fly ash cement concrete containing high volume bagasse ash. Journal of Building Engineering. 2020 Sep 1;31.
32. Gao Y, Jing H, Fu G, Zhao Z, Shi X. Studies on combined effects of graphene oxide-fly ash hybrid on the workability, mechanical performance and pore structures of cementitious grouting under high W/C ratio. Constr Build Mater. 2021 Apr 26;281.
33. Kaur R, Kothiyal NC, Arora H. Studies on combined effect of superplasticizer modified graphene oxide and carbon nanotubes on the physico-mechanical strength and electrical resistivity of fly ash blended cement mortar. Journal of Building Engineering. 2020 Jul 1;30.
34. Sabitha D, Dattatreya JK, Sakthivel N, Bhuvaneshwari M, Sathik SAJ. Reactivity, workability and strength of potassium versus sodium-activated high volume fly ash-based geopolymers. In: Current Science. 2012; 1320–7.
35. Smirnova OM. Compatibility of portland cement and polycarboxylate-based superplasticizers in high-strength concrete for precast constructions. Magazine of Civil Engineering. 2016;66(6):12–22.
36. Amran M, Fediuk R, Murali G, Avudaiappan S, Ozbakkaloglu T, Vatin N, et al. Fly ash-based eco-efficient concretes: A comprehensive review of the short-term properties. Materials. 2021 Aug 1;14(15).
37. Topark-Ngarm P, Chindaprasirt P, Sata V. Setting time, strength, and bond of high-calcium fly ash geopolymer concrete. Journal of Materials in Civil Engineering. 2015;27(7):04014198.
38. Rachman A, Aulia TB, Fauzi A, Syahyadi R, Amalia Z, Rosnita L. Feasibility of nagan raya power plantation waste as base material on geopolymer system. Key Eng Mater. 2021;87:51–6. Available from: www.scientific.net
39. Chajec A, Chowaniec A, Królicka A, Sadowski Ł, Żak A, Piechowka-Mielnik M, et al. Engineering of green cementitious composites modified with siliceous fly ash: Understanding the importance of curing conditions. Constr Build Mater. 2021 Dec 27;313.
40. Amran M, Debbarma S, Ozbakkaloglu T. Fly ash-based eco-friendly geopolymer concrete: A critical review of the long-term durability properties. Constr Build Mater. 2021 Nov 25;270.
41. Saidi T, Hasan M. The effect of partial replacement of cement with diatomaceous earth (DE) on the compressive strength and absorption of mortar. Journal of King Saud University - Engineering Sciences. 2022 May 1;34(4):250–9.
42. ASTM. Standard Practice for Mechanical Mixing of Hydraulic Cement Pastes and Mortars of Plastic Consistency. 2009;C305:1–3. Available from: www.astm.org
43. ASTM. Standard Test Method for Flow of Hydraulic Cement Mortar. 2001.
44. ASTM. Standard Test Methods for Time of Setting of Hydraulic Cement by Vicat Needle. 2010; (C191 – 08): 1–8.